Available online at www.sciencedirect.com
ScienceDirect
Journal of Sound and Vibration 325 (2009) 106–121
JOURNAL OF SOUND AND VIBRATION
www.elsevier.com/locate/jsvi

Experimental study on unsteady wake impacting effect in axial-flow compressors

Zhi-ping Li[a,*], Qiu-shi Li[a], Wei Yuan[a], An-ping Hou[a], Ya-jun Lu[a], Yu-lin Wu[b]

[a]*Chinese National Key Laboratory of Aerodynamics & Thermodynamics of Aeroengine, Beijing University of Aeronautics and Astronautics, Beijing 100191, PR China*
[b]*Department of Thermal Engineering, Tsinghua University, Beijing 100084, PR China*

Received 21 November 2006; received in revised form 20 May 2008; accepted 7 March 2009
Handling Editor: L.G. Tham
Available online 29 May 2009

Abstract

In the present study, the specific wake impacting effect (WIE) in compressors was used to control unsteady separated flows inside axial-flow compressors. Time-averaged performances were analyzed, key factors affecting the positive effects of WIE were studied and perspectives of engineering applications were discussed. Experiment results showed that when the compressor was working under near stall conditions, separated flows over rotor blade rows could be remarkably suppressed by utilizing WIE and properly adjusting two important parameters of impacting frequency and impacting intensity (wake defect). Under near stall condition, the flow-field structure inside the compressor was significantly improved and time-averaged performances were boosted, e.g. when $\bar{n} = 85\%n_0$ the total pressure increment was increased by 5.4%, the efficiency of the compressor was increased by 5.5% and the stall margin was increased by 30.7% under the condition of optimal impacting frequency and optimal impacting intensity.

0. Introduction

The staggered arrangement of rotor blade rows/stator blade rows in axial compressors means that there is strong unsteadiness inside compressors even under design condition, the wake shedding and motions of the upstream blade rows will exert periodic impacts on the downstream blade rows [1]. In comparison with airfoils, the profiles of compressor blades tend to create larger separation area and stronger vortex shedding, resulting in unsteady multimode flows with different sizes, different frequencies and different patterns. These modes and the interactions between them are closely related to the efficiency and maximum stage load of the compressor, and become the focus of recent studies.

Since 1994, Sharma et al. have studied the influences of time sequential effect on the efficiency of turbines, and pointed out that when stator/stator or rotor/rotor of the turbine situated in different relative circumferential position, the turbine efficiency would have a change of 0.5–1% or so [2]. Saren et al. studied

*Corresponding author. Tel.: +861082316862.
E-mail address: Leezip@buaa.edu.cn (Z.-p. Li).

0022-460X/$ - see front matter © 2009 Published by Elsevier Ltd.
doi:10.1016/j.jsv.2009.03.025

Nomenclature

A	passage area
A_1	maximum amplitude of the wake impacting
A_2	minimum amplitude of the wake impacting
A_e	average amplitude of the wake impacting
$\bar{A}_e$	relative amplitude of the wake impacting
b	chord
c	thickness at the blade trailing edge
c_{max}	maximum thickness of the blade
$\bar{c}$	relative thickness at the blade trailing edge
$\bar{d}$	hub/tip radius ratio
D	the diameter of case
f_e	external acoustic excitation frequency
f_{shed}	vortex shedding frequency
$\bar{f}_e$	relative excitation frequency $\bar{f}_e = f_e/f_{shed}$
h	blade height
l	integer
m	integer
n	rotate speed
$\bar{n}$	correct rotate speed
p	static pressure
P^*	total pressure
P^*_{loss}	total pressure losing of wake generator
Q	volume flux
SM	stall margin
S_t	S_t number
v	velocity of the flow
v_{main}	velocity at the mainstream
v_{wake}	velocity at the wakestream
Z_s	the number of inlet guide vane
δ	coefficient of the relative increment
Δ	coefficient of the absolute increment
$\Delta\beta^*$	bending angle of rotor blades
$\Delta\beta_{\max}$	the maximum bending angle of rotor blades
η^*_{st}	compressor stage efficiency
ρ	density of the atmosphere

Superscript and subscript

0	parameters under design condition
1	parameters at the inlet
2	parameters at the exit
i	total pressure rake measurement point
s	parameters under stall condition

the influences of time sequential effect on the time-averaged performances of turbines [3–6]. The results indicated that the time sequential effect had certain influences on turbine efficiency, whereas it had only a little effect on compressor efficiency; in particular, it had little positive effect in the case of low speed axial-flow compressors [7]. Hence questions arise whether the interference between rotor/stator has effects on the time-averaged performance of compressors and how much is the potential underlying in the inherent unsteady flows?

The theory of the third generation of unsteady flow types was proposed in aerodynamics, in which the key was wave-vortex resonance, i.e. unsteady excitations were utilized to control the evolution and development of separated shear layers so that disordered free separated flows could be transformed into periodic or quasi-periodic ordered flows and the lift be increased and the drag be decreased. In 2001, Prof. Zhou and his group started the researching about interaction of unsteady separated flow over multi-bodies moving relatively in the same flow field by CFD simulation on a single-stage low-speed axial flow compressor and experimental investigations on a stationary annular cascade wind tunnel, and proposed firstly the new theory of unsteady cooperative flow type (UCFT). Authors pointed out that the time–space structure of unsteady separated flow field can be remarkably improved and the time-averaged aerodynamic performance can be significantly enhanced if the new flow type—UCFT can be realized [8]. But so far, most of studying was numerical simulation or model experiment, and did not be investigated in real compressors. The present paper will carry out the detailed experimental investigation about UCFT in a real axial-flow compressor facility.

As for unsteady separated flows inside axial-flow compressors, the wakes of upstream blade rows have impacting effects on the time–space structure of unsteady separated flows over downstream blade rows, which are defined as 'wake impacting effect (WIE)'. From the viewpoint of wave-vortex resonance, here unsteady excitation sources are ready-made, and demands and opportunity for restraining separation regions are also existent. It is reasonable to expect that once the interaction between the upstream wakes and the downstream

vortex shedding can be properly controlled, the flow field structure of compressors can be improved and the time-averaged performances be increased.

Experiments were carried out in our experimental facility of one-stage low-speed axial compressor; a special facility—wake generator was designed to study the influences of unsteady impacting effect of wakes on time-averaged aerodynamic performances and the stability of unsteady flow. The effects of impacting frequency and impacting intensity were also studied, and it was found that both the time-average performances and the stall margin were significantly improved under optimal conditions.

1. Simplified WIE model

For utilizing WIE to work out the potential of unsteady flow inside compressors, the key point is to implement the coupling between the impacting frequency of upstream wakes and the characteristic frequency of vortex shedding in the unsteady flows over downstream rotor blades. In some sense, WIE is interaction between the upstream stator and the downstream rotor. It is very difficult to capture such unsteady coupling even in an experimental facility of single stage compressor, since it requires a series of changes in geometric and aerodynamic parameters and it is very difficult to analyze and optimize any single parameter separately. Thus a simplified WIE model was proposed in the present paper, in which the match and optimization between the exit boundary condition of the stator blade row and the inlet boundary condition of the rotor blade row was used to capture and embody the WIE. Please refer to Ref. [9] for detail.

1.1. Mathematic model of the boundary condition at the exit of the stator

The wake distribution at the exit of stator domain was assumed to be periodic along the circumferential direction, the distributions of all aerodynamic parameters can be determined along the circumferential direction on S3 surface. When the periodic impacting of the wakes of stator blades on the downstream rotor blades was studied, what should be done was to transform the circumferential distributions of aerodynamic parameters on S3 surface at the exit onto the rotor domain, then the inlet boundary conditions were obtained for the rotor domain, i.e. transformation from the absolute coordinate system to the relative coordinate system.

First, the incoming flow was assumed to be steady and the period for the variables was

$$q(\theta) = q\left(\theta + \frac{2\pi}{Zs}m\right) \tag{1}$$

where $1 \leqslant m \leqslant Zs$ and Zs denoted the number of the stator blades. Eq. (1) could be transformed into exponential form by Fourier expansion as follows:

$$q(\theta) = \sum_{-\infty}^{\infty} C_m e^{imZs\theta}, \quad m = 0, \pm 1, \pm 2, \ldots \tag{2}$$

The strong reversal pressure gradient inherent in the stator domain made the equation strong nonlinear, which had two variables (θ and t) as follows:

$$q(\theta) = \sum_{l=-\infty}^{\infty} \sum_{m=-\infty}^{\infty} C_l^m e^{im\omega t} e^{ilZs\theta}, \quad l, m = 0, \pm 1, \pm 2, \ldots \tag{3}$$

In which ω was the main frequency of the frequency spectrum of the unsteady separated flows downstream of the stator.

1.2. Mathematic model of the boundary condition at the inlet of the rotor

The following transformation from the absolute coordinate system into the relative coordinate system was introduced

$$\theta = \varphi + \Omega t \tag{4}$$

In which Ω was the rotating speed (angular velocity) of the rotor, and was assumed to be steady and constant. Inserting Eq. (4) into Eq. (2), we obtained

$$q(\varphi,t)=\sum_{m=-\infty}^{\infty}C_m e^{imZs(\varphi+\Omega t)}=\sum_{m=-\infty}^{\infty}C_m e^{imZs\varphi}e^{imZs\Omega t},\quad m=0,\pm1,\pm2,\ldots \tag{5}$$

Inserting Eq. (4) into Eq. (3), we got

$$q(\varphi,t)=\sum_{l=-\infty}^{\infty}\sum_{m=-\infty}^{\infty}C_l^m e^{im\omega t}e^{ilZs(\varphi+\Omega t)}=\sum_{l=-\infty}^{\infty}\sum_{m=-\infty}^{\infty}C_l^m e^{ilZs\varphi}e^{i(lZs\Omega+m\omega)t},\quad l,m=0,\pm1,\pm2,\ldots \tag{6}$$

Eq. (5) showed that when there was no obvious vortex shedding in the wakes downstream of the stator, the latter could be considered as a steady one, i.e. $\omega=0$. There existed at the rotor inlet several traveling waves rotating around the downstream rotor blades with angular velocities of ($mZs\Omega$) in the relative coordinate system. Eq. (6) indicated that when there was large scale separated flow over the stator, there would be obvious vortex shedding in the wakes, the main frequency of which was ω, and there would be at the inlet of rotor domain several traveling waves rotating around the downstream rotor blades with angular velocities of ($mZs\Omega+n\omega$) in the relative coordinate system. In comparison with Eq. (5), the traveling waves or the modes of the traveling waves were changed.

Unsteady WIE was nothing but a 'wave-vortex coupling' interaction between the rotating traveling waves caused by the wakes of upstream stator blades and the unsteady vortex shedding in the unsteady flows over downstream rotor blades. Optimization and matching of the aerodynamic arrangement along the circumferential direction could properly organize this 'wave-vortex coupling' interaction, increase time-averaged performances and improve the stall margin.

2. Experimental facilities

2.1. Low-speed axial-flow compressor

The investigations are conducted on a single-stage low-speed axial flow compressor. Fig. 1 shows the schematic diagram of the experimental facility, and the design specifications are listed in Table 1. As show in Fig. 1, the blade profile of both the rotor and the stator vane is C4. The design specifications of the rotor blade and the stator vane are listed in Table 2. The design mass flux and total pressure-rise between inlet total pressure and exit total pressure are 2.40 m^3/s and 1500 Pa, respectively (Fig. 2).

Since our purpose of study was underlying mechanism rather than actual flow field inside the compressor. Hence, the bending angle was artificially enlarged ($\Delta\beta^*/\Delta\beta_{max}$ was as large as 0.95) in our design, so that the flow separation could be amplified and large scale vortex shedding could be observed.

2.2. Generator of unsteady wakes

In order to simulate the wake impacting effects inside actual compressors, we designed a specific generator of unsteady wakes, in which the profile was chosen by referring to Ref. [9], as shown in Fig. 3.

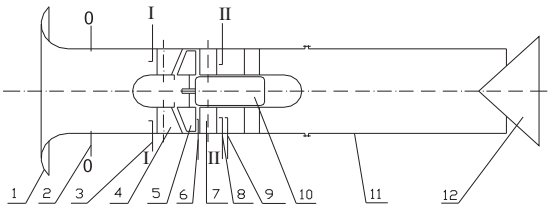

Fig. 1. Schematic diagram of low-speed axial-flow compressor: (1) flow gathering ware, (2) front casing static pressure holes; (3) inlet total pressure comb, (4) inlet guide vane, (5) rotor blade, (6) Kulite total pressure probe, (7) stator blade, (8) outlet total pressure comb, (9) outlet total pressure rake, (10) generator, (11) rear casing, and (12) throttle plug.

Table 1
Design specifications of low-speed axial-flow compressor.

Design parameters	Value
Rotor tip diameter (mm)	450
Rotor tip speed (m/s)	70.7
Hub/tip ratio	0.75
Number of rotor blades	19
Number of stator vanes	13
Rotor tip clearance (% of rotor tip chord)	0.7

Table 2
Design specifications of rotor blade and stator vane in low-speed axial-flow compressor.

	Rotor	Stator
Solidity	0.605	0.671
Stagger angle (°)	34.49	79.85
Max thickness (% of tip chord)	9.50	7.10

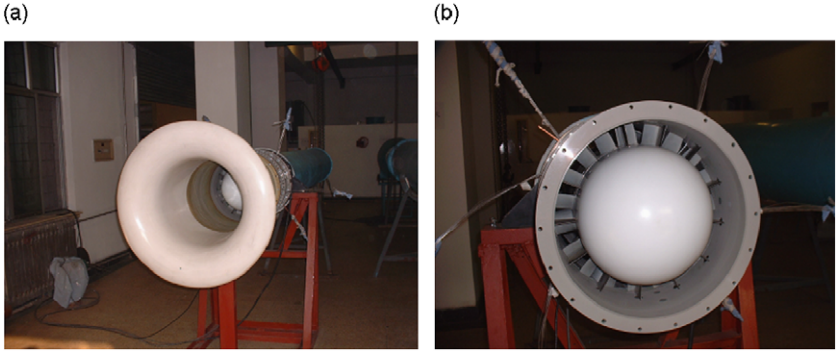

Fig. 2. Photo of the experimental facility: (a) overall view and (b) experimental section.

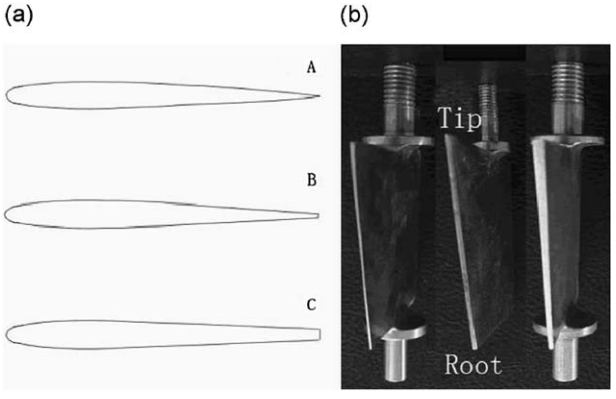

Fig. 3. Blades of wake generator: (a) middle section and (b) photo of blades.

The blade was chosen to be a straight one, and the thickness at trailing edge can be adjusted to generate wakes with proper impacting intensities (wake defects), which were chosen by referring to [9]. Three profiles were designed with different relative thickness at the trailing edge ($\bar{c} = c/c_{\max}$), i.e. 16.7%, 39.1% and 70.4%, respectively. In the present generator, the number of blades can be arranged in 25 different combinations from

100 to 4800 Hz. in other words, the impacting frequency can be easily adjusted. Fig. 4 shows the photo of the wake generator.

2.3. Measurement system and measurement scheme

L-type dynamic total pressure probes were used, in which Kulite XCQ-093 micro pressure sensors were installed. Please refer to Table 3 for their specific parameters. The dynamic total pressure probes were installed on a movable rotordate with two dof, its radial position and axial angle could be easily adjusted. The locations for dynamic measurements were shown in Fig. 1; the holes for installing the probe were between the stator and the rotor with a distance of 8% b to the trailing edge of the rotor.

In the present steady measurement system, steady pressure sensors with three different ranges were adopted for measuring different parameters, such as total pressure at the inlet, static pressure at the inlet and total pressure at the exit, with specific parameters given in Table 4.

The section for measuring the flow rate was shown as '2' in Fig. 1, there were four small static-pressure holes distributing along the circumferential direction, steady pressure sensors were used to measure the static pressures p at the inlet (pressure difference) with a precision of err <10 Pa.

The total pressures at the inlet P_1* were measured by 5-hole total pressure comb, 5 channels were equally distributed along the radial direction and the section for measurement was shown as 'I-I' in Fig. 1.

The total pressures at the exit P_2* were measured by a 25-hole total pressure rake, which covered 1.1 cascade passages and were distributed along the circumferential direction at the axial position of 10% b as

Fig. 4. Photo of wake generator.

Table 3
Specification of Kulite dynamic pressure sensor.

Model	Full scale (PSI)	Working temperature (°C)	Inherent frequency (KHz)	Precision (%FS)
XCQ-093	1	−55 to 204	100–120	0.1

Table 4
Parameters of the steady pressure sensors.

Model	Parameters	Full scale (mmH_2O)	Quantity	Precision (%FS)
163PC01D75	p_1^*	20	5	0.25
DRAL501DN	p	60	1	0.25
AM5302 DV	p_2^*	200	25	0.25

indicated by '5' in Fig. 1. The total pressure rake was installed on a movable rotordate with two dof, and could be adjusted to measure flow parameters at several radial locations.

3. Experiment results and discussion

Emphases of the experiments were laid on the influences of WIE on the time-averaged performances and the stall margin of the compressor, as discussed in the following.

3.1. Dynamic experiments

In earlier experiments we found out that the impacting frequency had great effects on the time-averaged performances and was closely correlated with the unsteady characteristic frequency in the outlet flow field of the rotor. Hence we must first carry out detail study on the unsteady characteristic frequency in the outlet flow field of the rotor. In Ref. [11] the author carried out detail dynamic measurements in the outlet flow field of the rotor, and captured the characteristic frequency of unsteady vortex shedding. We found out in acoustic excitation experiments that, when the non-dimensional excitation frequency equaled one, the efficiency, the total pressure increment and the stall margin of the compressor were all increased, meanwhile the internal flow field was improved and the unsteady separation was effectively restrained, and the present experimental study was planned based on these conclusions. The present results will be compared with and verified against these results so that the physical mechanism underlying WIE can be revealed.

3.2. Experiments of unsteady wake impacting

3.2.1. Analysis of the intensity of the wake impacting

The numerical simulations of Ref. [9] regarding unsteady WIE in compressors showed that the intensity of the unsteady wake impacting had strong influences on the impacting effects, when the intensity was less than 30%, the WIE had little effects on the time-averaged performances of the compressors, when the intensity was greater than 30%, i.e. when it exceeded certain threshold, the time-averaged performances of the compressors, such as efficiency and pressure ratio, would be improved as long as the impacting frequency was within certain range.

The distribution of the wakes behind the mid-section profile was measured by a total pressure rake with 13 holes, as shown in Fig. 5. In which, the coordinate x was the total pressure rake's measurement position; coordinate y was the total pressure losing P^*_{loss} at the wake generator's outlet.

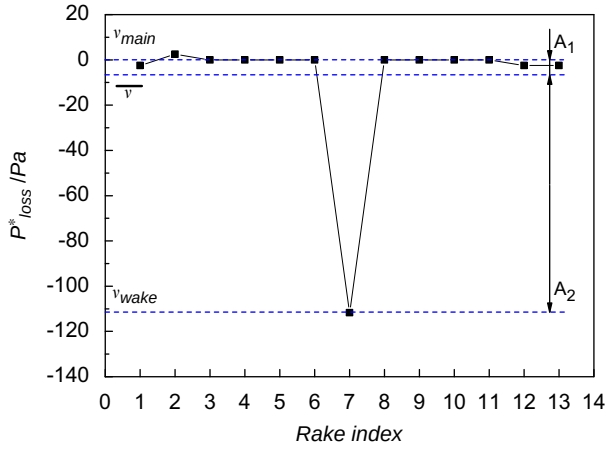

Fig. 5. Distribution of the wake behind the profile (Blade B).

Table 5
Relativity intensity of unsteady wake.

v_{main} (m/s)	$\bar{A}_e$ (%)		
	Blade A	Blade B	Blade C
39.7	26.9	34.6	40.5
35.1	27.5	34.9	41.5
26.9	29.2	35.8	43.1

In our study, the air flow is axial direction and is incompressible flow, so we can estimated the flow velocity through the measuring tatol pressure losing and can get the intensity of wake impacting by the velocity distribution at the generator's outlet too, as shown in Eq. (7).

$$\begin{cases} \bar{v} = \sum_{i=1}^{13} v_i \Big/ 13 \\ A_1 = v_{main} - \bar{v} \\ A_2 = v_{wake} - \bar{v} \\ A_e = \dfrac{A_2 - A_1}{2} = \dfrac{v_{wake} - v_{main}}{2} \\ \bar{A}_e = \dfrac{A_e}{\bar{v}} = \dfrac{v_{wake} - v_{main}}{2\bar{v}} \times 100\% \end{cases} \tag{7}$$

where v_i is the velocity at the different measurement points, $\bar{v}$ the average velocity of outflow, v_{main} the velocity at mainstream, and v_{wake} the velocity at wakestream. A_1, A_2 are peak amplitude and the bottom amplitude of the wake impacting. A_e is the average amplitude of wake and $\bar{A}_e$ the non-dimensional amplitude. In real compressor, the wake width was larger than this generator's wake, so the difference between peak amplitude and bottom amplitude of the wake was almost equal. To make the experimental results universally applicable, average amplitude and non-dimensional amplitude have been choice in this paper.

Using Eq. (7), we know that the wake relativity intensity of three generators and the values are given in Table 5.

From Table 5, we know that the intensity of blade B is closer to the threshold value 30%, so we selected the second blade in our experiment investigation.

3.2.2. The influences of WIE on time-averaged performances

Based on the above dynamic experiments and the conclusions drawn from the acoustic excitation [10] and according to the idea of 'wave-vortex coupling', the coupling between the impacting frequency and the characteristic frequency of vortex shedding was first studied.

In relative coordinate system, the wakes generated by the generator would pass the rotor blade row consecutively, i.e. would impact the rotor blade row with certain frequency, the converted frequency could be calculated by Eq. (8).

$$f_e = Zs\frac{n}{60} \tag{8}$$

To make the results universally applicable, all parameters were non-dimensional and defined by the following equation.

$$\bar{f}_e = f_e/f_0 \tag{9}$$

The purpose of our research is to investigate the cooperative effect between upstream wakestream and downstream unsteady separative flow. So we only care about the vortex shedding frequency which shed from rotor blade. In Eq. (9), f_0 is the basic frequency of the characteristic frequency of unsteady separation vortex. It could be experimented by dynamic Kulite probe at the rotor blade outlet, the results could be concluded by the criterion given in Ref. [11] and the present study that $f_0 = 1854$ Hz.

Emphasis of the present experiments was laid on changes of the time-averaged performances when the working condition varied from the design point to the stall. The main reason is as follows. The key point is the

coupling or the interaction between wave and vortex; however, under small incidence there will not be large separation, even no separation, around the downstream rotor. Hence there will be little coupling effect resulting from WIE under small incidence, which was clearly demonstrated in the present study.

The time-averaged performances under three different impacting frequencies were given and compared in Fig. 6, in which the coordinate x was the correct mass flux Q_{cor}, coordinate y was the efficiency η^* and the total pressure-rise ΔP^*, respectively. Black curve denoted the performances of unexcited case, whereas the red curves represented the performances under wake impacting. It could be seen from the figure that the unexcited efficiency was measured to be 83.5%; about 1.5% lower than the designed value 85%, resulting from the following three causes. First, the design does not take the clearance around the blade tip into consideration;

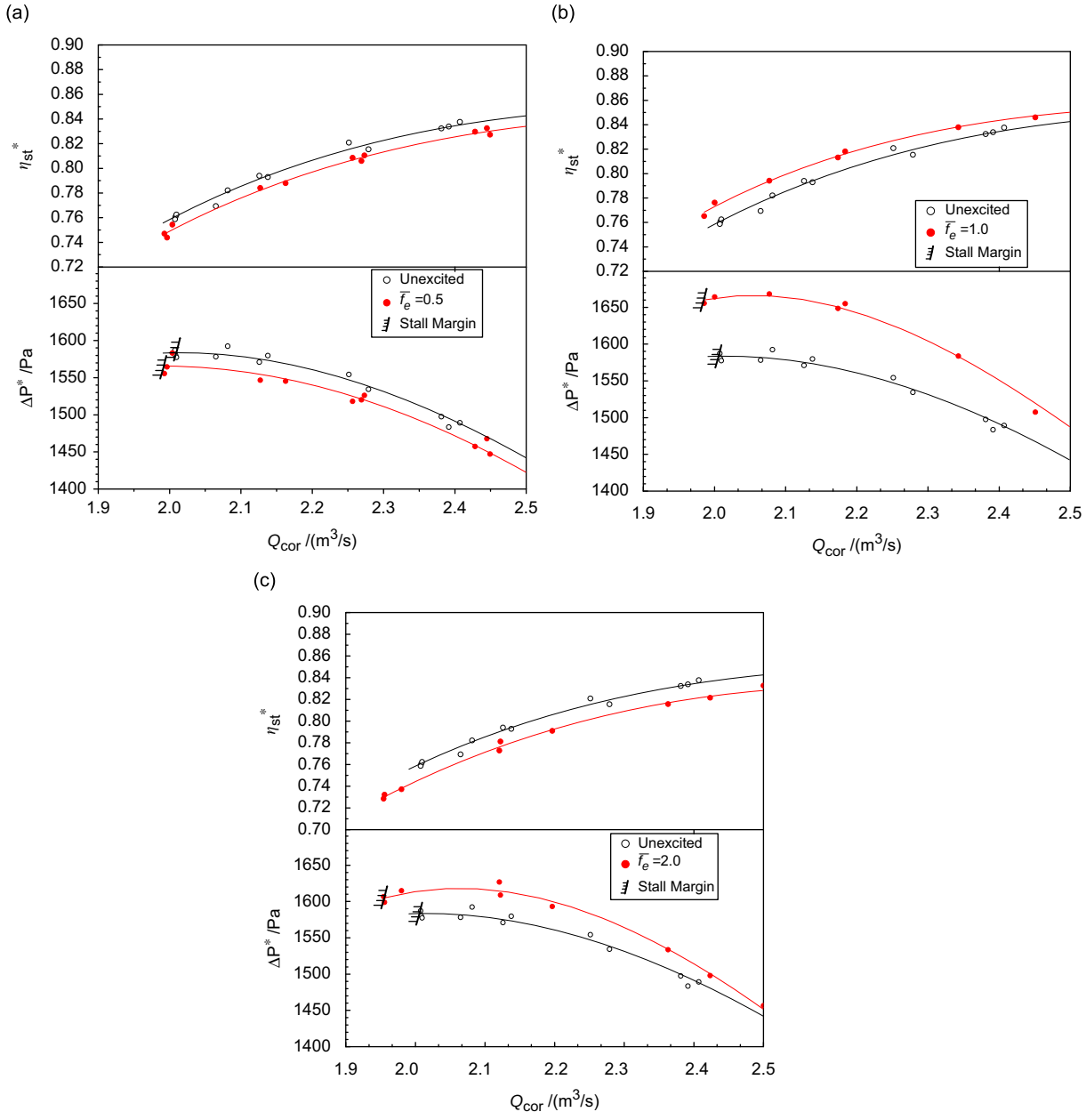

Fig. 6. Influence of wake impacting frequency on aerodynamic performances: (a) $\bar{f}_e = 0.5$, (b) $\bar{f}_e = 1.0$, and (c) $\bar{f}_e = 2.0$.

hence the experimental result would be worse than the design value. Secondly, a mechanical accident occurred during adjustment and calibration and led to damage in rotor blade tip, after polishing the clearance became even larger, thus the efficiency would become lower. However, the main approach adopted in the present study is to compare the aerodynamic performances with and without the wake impact effect, hence a little change in efficiency will not affect our experiment results and discussion, and our efforts will be focused on the relative changes of efficiency (η^*), total pressure [$\delta(\Delta P^*)$] increment and stall margin (SM).

In all the above-mentioned cases with three different impacting frequencies, the compressor's aerodynamic performances exhibited clear changes; in particular, they were greatly improved near the stall. The experiments were carried out as follows. Kulite dynamic pressure probes were used to monitor the distribution and evolution of pressure wave at the rotor exit (their radial locations were 72 and 40%h, respectively), and the flow passages were monitored at the same time. The evolution of pre-waves could thus be accurately captured and the flow-rate at the stall could be measured. A typical monitor results were shown in Fig. 7, in which A and B gave the dynamic measurement at 72 and 40%h, respectively, and the measurement of flow rate was presented in C.

The stall margin could be calculated by the following equation:

$$SM = \left(\frac{\Delta P_s^*/Q_s}{\Delta P_0^*/Q_0} - 1\right) \times 100\% \tag{10}$$

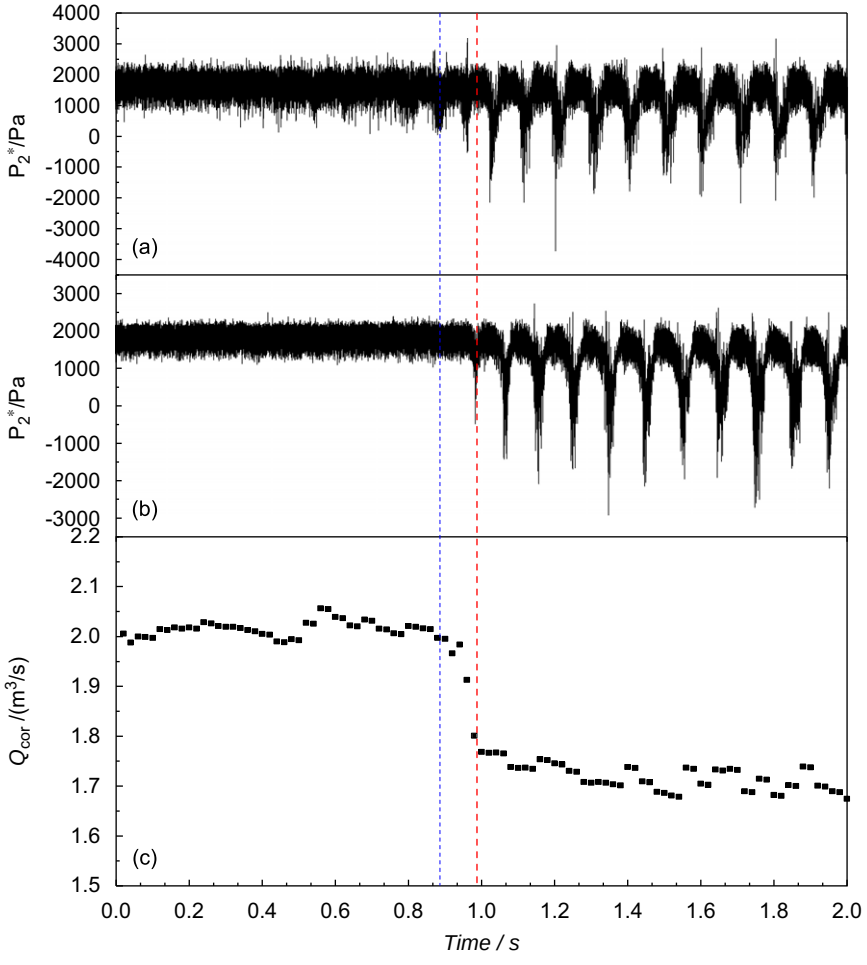

Fig. 7. Monitor of the stall.

In which the subscript's' denoted the parameters under stall condition, whereas the subscript '0' denoted parameters at the design point. The aerodynamic parameters under stall condition were concluded from the experiments as follows. $Q_s = 2.0\,m^3/s$, $\Delta P_s^* = 1579\,Pa$, and $\eta_s^* = 75.9\%$. The stall margin under steady inlet condition could be calculated from Eq. (10) to be 26.1%.

Table 6 gave the influences of WIE on the relative increment of efficiency, total pressure-rise and stall margin at $Q_s = 2.08\,m^3/s$. The variations of time-averaged performances, such as efficiency, total pressure increment and stall margin, with the impacting frequency were shown in Figs. 8 and 9. Blue curves denoted the standard performances under steady flow condition, whereas red curves displayed variations of the time-averaged performances vs. the impacting frequency.

Table 6
Influence of WIE on performances of the compressor.

$\bar{f}_e$	$\delta(\Delta P^*)$ (%)	$\delta\eta^*$ (%)	δSM (%)
0	0.0	0.0	0.0
0.25	−0.38	−1.28	2.3
0.375	2.26	−0.51	11.9
0.5	−1.38	−1.53	0.4
0.6	2.14	0.13	10.3
0.75	3.58	0.64	12.3
0.9	2.95	0.38	18.8
1.0	4.52	1.53	24.9
1.2	3.02	0.38	12.3
1.5	1.88	−1.40	10.0
1.8	0.88	−1.53	6.1
2.0	2.07	−2.04	16.7
2.4	−0.38	−3.45	1.9

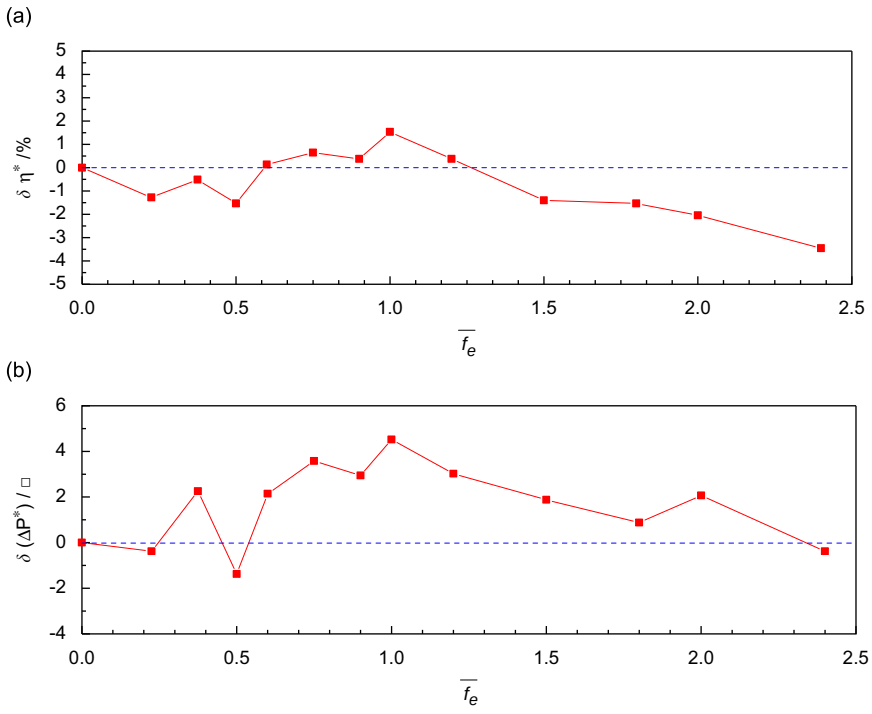

Fig. 8. Variations of performances of the compressor vs. the impacting frequency at $Q_{cor} = 2.08\,m^3/s$: (a) relative efficiency and (b) relative pressure ratio.

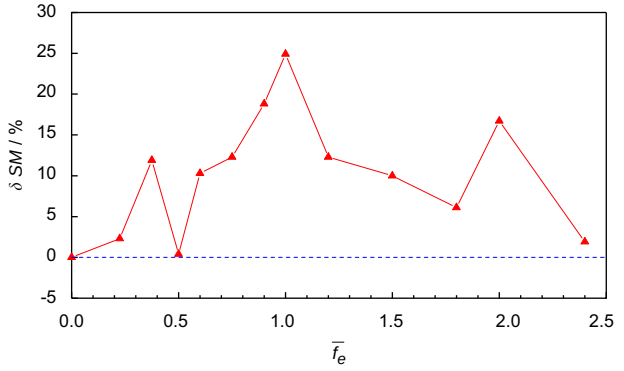

Fig. 9. Variations of the stall margin vs. the impacting frequency.

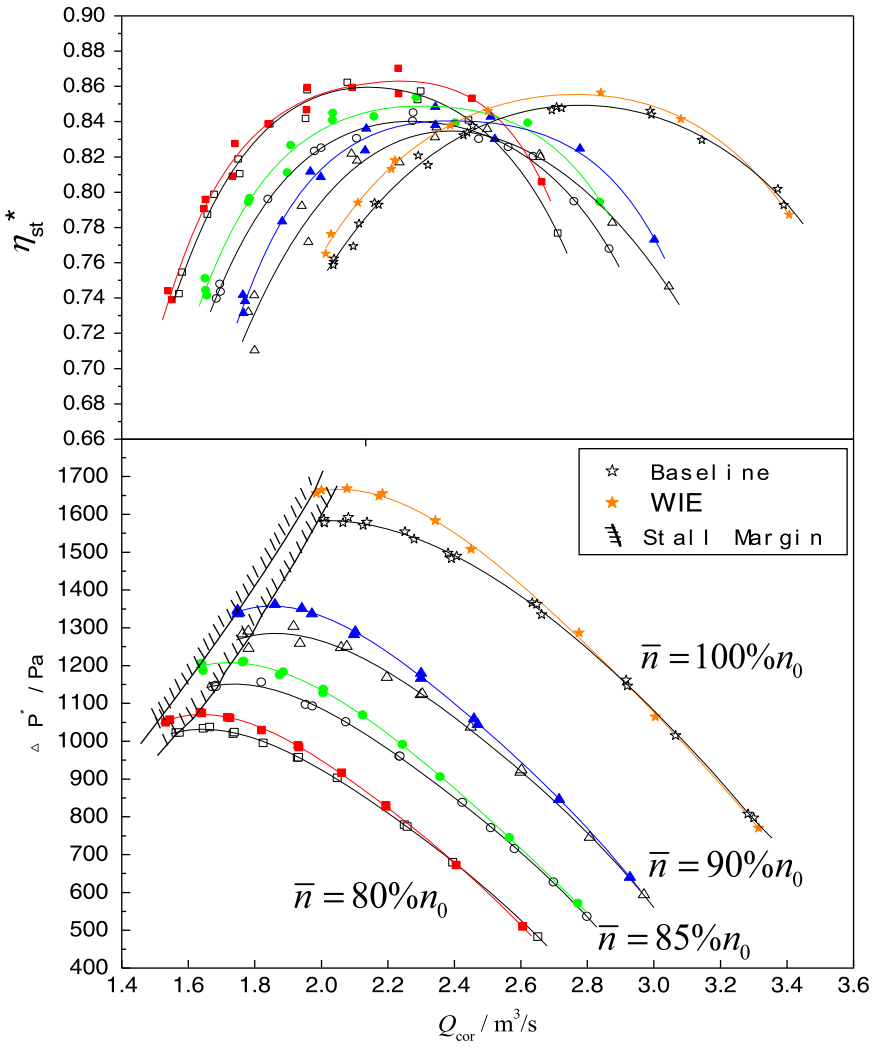

Fig. 10. Influence of the compressor's rotating speed on WIE.

It could be seen from Fig. 8(a) and (b) that the total pressure increment was increased in all three cases. However, its influence on the efficiency was different. When the efficiency and the total pressure increment were considered comprehensively, the range of impacting frequency for effective wake impacting effect could be concluded as the range between the two blue vertical lines shown in Fig. 8. In other words, when $\bar{f}_e = 0.375$ and $0.6 \leqslant \bar{f}_e \leqslant 1.2$, the efficiency remained nearly the same but the total pressure increment was greatly increased, in which when $\bar{f}_e = 0.75$, the total pressure increment was increased to the utmost. On the other hand, when $\bar{f}_e > 1.2$, although the total pressure increment was still increased to some extent, however the efficiency was obviously deteriorated, hence we concluded that the WIE did not bring about coupling effect in this case, and no improvement could be observed in the compressor performances.

It could be seen from Fig. 9 that there occurred three peaks, i.e. $\bar{f}_e = 0.375, 1.0, 2.0$, in the variation curve of stall margin vs. impacting frequency, among which the maximum was 5.14% corresponding to $\bar{f}_e = 1.0$. It is interesting to point out that if $\bar{f}_e = 1.0$ is taken as the best impacting frequency—the basic frequency, then the two peak frequencies of 1.0 and 2.0 reveal a relationship of double frequency. On the other hand, it can be seen from both Figs. 8 and 9 that the time-averaged performances corresponding to $\bar{f}_e = 0.5$ are deteriorated, i.e. when the impacting frequency equals half of the basic frequency, the impacting effect leads to bad results. Therefore, although an apparent bump occurs at the location $\bar{f}_e = 0.375$, the reason is nothing but the decline of performances near $\bar{f}_e = 0.5$, and thus the first peak is not a real peak.

3.2.3. *Influence of the compressor's rotating speed on WIE*

All the above experiments were carried out under the condition of $\bar{n} = 100\%n_0$. However, the actual compressors often worked with different rotating speed, usually with 80–90%n_0. This problem was also studied.

The number of the blades was kept unchanged, i.e. the impacting frequency 2000 Hz was unchanged, the rotating speed was controlled to be 100, 90, 85, and 80%n_0, and the respective performances were obtained and shown in Fig. 10. Here hollow circles represented the unexcited performances with steady incoming flow, whereas the solid circles represented the performances under WIE and different rotating speed. It could be concluded from Fig. 10 that all the performances under WIE and different rotating speed showed positive effects, in particular, they were much improved near the stall, which was compatible with the conclusion drawn in above sections. This can be explained based on the following definition of S_t number.

$$S_t = \frac{f_0 D}{u} \tag{11}$$

In which f denoted the unsteady frequency of vortex shedding ($f = f_0$), D is the characteristic geometric length of the profile, u is the axial averaged velocity of the incoming flow. As for a definite engine, we can assume S_t is a constant, and D is a constant too, so f_0 is proportional to u, wake frequency f_e scale with rotor speed. On the other hand, the non-dimensional wake frequency scale with f_e and scale inversely with f_0. Once the optimal wake impacting frequency is determined, the $\bar{f}_e$ is a constant always and will be 'locked-in' with regard to the number of blades no matter whether the rotating speed is changed as long as the impacting intensity is larger than the threshold. However, the impacting intensity would decrease with decreasing rotating speed, and if the latter decreased to become less than a certain threshold, the impacting intensity would be lower than the threshold and there would not be positive effects as shown in Fig. 10. When $\bar{n} = 80\%n_0$, the positive effects were not quite distinct.

As shown in Fig. 10, when $\bar{n} = 85\%n_0, 90\%n_0$, the compressor's performances were all greatly improved. The efficiency, total pressure increment and stall margin were all increased under optimal impacting conditions, as given in Table 7.

For evaluating the positive effects of WIE on the compressor's time-averaged performances, the following approach was adopted. First, the efficiency, total pressure increment and stall margin were chosen as the parameters to be evaluated. Second, one of the above parameters was kept unchanged; the variations of the rest two were analyzed so that the best effect could be obtained.

First, the stall margin was analyzed, as shown in Fig. 11. The case of 85% designed rotating speed was chosen to be evaluated. Point A and A′ were the stall points with and without WIE respectively. In order to keep the stall margin unchanged, we must make $SM_1 = SM_2$. Thus, only the time-averaged performances

Table 7
Influence of the rotating speed on WIE.

Operating model	$\bar{f}_e = 0$		$\bar{f}_e = 1.0$	
	SM (%)	SM (%)	ΔSM (%)	δSM (%)
$\bar{n} = 100\%n_0$	26.1	32.6	6.5	24.9
$\bar{n} = 90\%n_0$	28.9	34.9	6.0	20.2
$\bar{n} = 85\%n_0$	30.8	40.3	9.5	30.7
$\bar{n} = 80\%n_0$	31.0	35.5	4.5	14.5

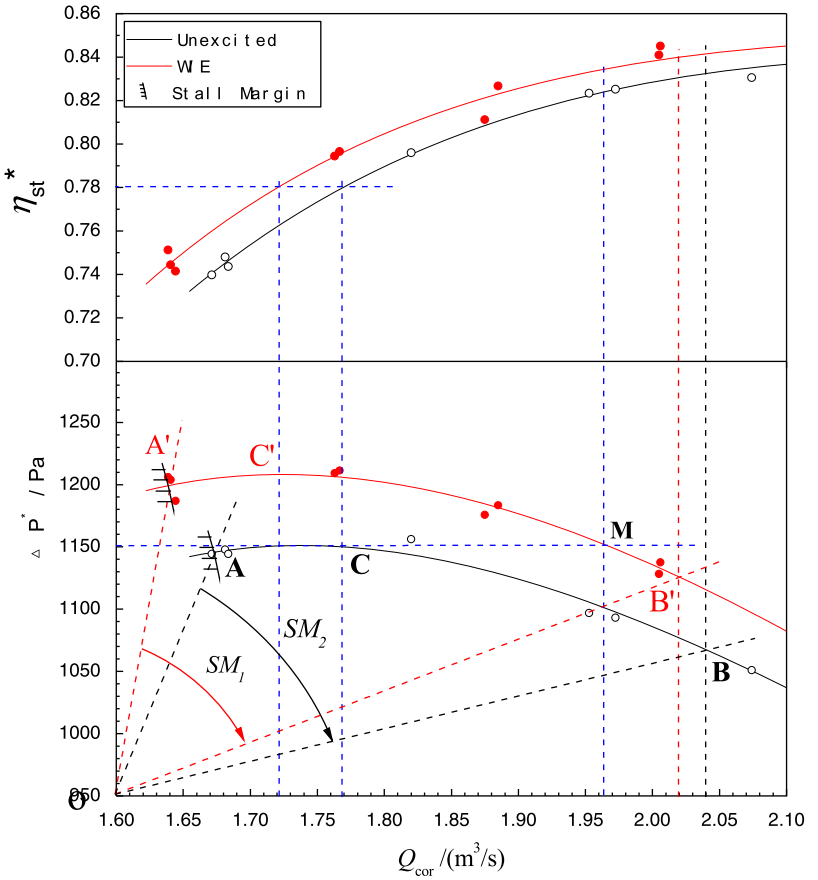

Fig. 11. Influence of WIE on time-averaged performances, when $\bar{n} = 85\%n_0$.

under working condition of B and B′ need to be evaluated. Second, keep the total pressure increment unchanged as shown in Fig. 11, the maximum (point C) of the performance was chosen as the working condition with unchanged total pressure increment, thus the aerodynamic performances under working condition C and C′ should be compared. When the efficiency was kept unchanged, only the time-averaged performances under working condition of C and M need to be compared, as given in Table 8. In this case, the efficiency was increased by 5.4%, the total pressure increment was increased by 5.5% and the stall margin was increased by 30.7%.

It can be concluded from the above analysis that the change of the rotating speed within certain range will not influence the positive effects of WIE, and thus the engineering application of WIE is quite promising.

Table 8
Influences of WIE on time-averaged performances of the compressor when $\bar{n} = 85\%n_0$.

Performance par.	Unchanged SM		Unchanged η^*		Unchanged Δp^*	
	B	B'	C	C'	C	M
η^*_{st} (%)	83.2	84.0	78.1	78.1	78.1	83.5
$\delta\bar{\eta}$ (%)	–	0.8	–	–	–	5.4
ΔP^* (Pa)	1067	1126	1152	1209	1152	1152
$\delta(\Delta P^*)$ (%)	–	5.5	–	4.9	–	–
SM (%)	30.8	30.8	30.8	40.3	30.8	40.3
δSM (%)	–	–	–	30.7	–	30.7

4. Conclusion

A series of model experiments were carried out to study the unsteady wake impacting effect inherent in compressors. The present results showed that under properly adjusted impacting frequency and impacting intensity of the upstream wake, the downstream flow over rotor blade row could be made coupling with the upstream flow, and the upstream impacting could make the characteristic frequency of the downstream unsteady separated flow being 'locked-in', make the downstream flow field more orderly and increase the time-averaged performances. The conclusion could be summarized as follows.

1. When $\bar{n} = 100\%n_0$, the optimal wake impacting frequency was $\bar{f}_e = 1.0$. When the impacting intensity reached the threshold value (30%), the rotary traveling waves generated in the upstream flow over the stator blade row would be coupling with the unsteady vortex shedding in the downstream flow-field around the rotor blade row, so that the downstream separated flow was effectively restrained and the time-averaged performances and the stall margin were improved.
2. The range of impacting frequency for effective WIE was $0.6 \leqslant \bar{f}_e \leqslant 1.2$. When $\bar{f}_e = 1.0$, the time-averaged performances and the stall margin were improved most prominently.
3. The best impacting frequency for effective WIE did not vary with varied rotating speed of the compressor. However, the positive effects were influenced by the impacting intensity; they would not be exhibited if the intensity was lower than certain threshold. When $\bar{n} = 85\%n_0$, the positive effects would be most obvious: The relative increment of total pressure was increased by 5.4%, the efficiency of the compressor was increased by 5.5% and the relative stall margin was increased by 30.7%.

It can be concluded from the present experiments that there are significant potential inherent in the unsteady flows inside compressors, which has remarkable prospects in engineering applications.

Acknowledgment

The present study was carried out under the guidance of the new theory of unsteady cooperative flow type proposed by Prof. Zhou Sheng, and hopes to be able to serve as its experimental verification. The authors wish also to express their thanks to the National Natural Science Foundation for its financial support under the project number [50476003].

References

[1] L. Higenfeld, M. Pfitzner, Unsteady boundary layer development due to wake passing effects on a highly loaded linear compressor cascade, ASME Paper, GT2004-53186.

[2] F.W. Huber, P.D. Johnson, O.P. Sharma, et al., Improvement through indexing of turbine airfoils—part I: experimental investigation, ASME Paper No. 95-GT-27, 1995.
[3] V.E. Saren, N.M. Savin, D.J. Dorney, et al., Experimental and numerical investigation of unsteady rotor-stator interaction on axial compressor stage (With IGV) performance, *Proceedings of the Eighth International Symposium on Unsteady Aerodynamics and Aeroelasticity of Turbomachines*, Stockholm, Sweden, September 14–18, 1997.
[4] D.J. Dorney, O.P. Sharma, K.L. Gundy-Burlet, Physics of airfoil clocking in a high-speed axial compressor, ASME Paper No. 98-GT-82, 1998.
[5] G.J. Walker, J.D. Hughes, W.J. Solomon, periodic transition on an axial compressor stator-incidence and clocking effects—part1: experimental data, ASME Paper No.98-GT-363, 1998.
[6] S.T. Hsu, A.M. Wo, Reduction of unsteady blade loading by beneficial use of vortical and potential disturbances in an axial compressor with rotor clocking, *ASME Journal of Turbomachinery* 13 (2) (1999) 10–16.
[7] W.S. Barankiewicz, M.D. Hathaway, Effects of stator indexing on performance in a low speed multistage axial compressor, ASME Paper No. 97-GT-496, 1997.
[8] S. Zhou, X.-Q. Zheng, A.-P. Hou, Y.-J. Lu, Interaction of unsteady separated flow over multi-bodies moving relatively in the same flow field, *Journal of Sound and Vibration* 288 (2005) 981–1009.
[9] H. Anping, Investigation on Theory of Two Genarations Unsteady Flow Types in Axial Compressor, The thesis for doctorate in BUAA, 2003, p. 9.
[10] L. Zhiping, G. Zhiqiang, L. Yan, L. Yajun, The experiment research on the performance of low speed axial-compressor by external acoustic excitation, ASME Paper, GT2004-53183.
[11] L. Zhi-ping, L. Qiu-shi, Y. Wei, H. An-ping, L. Ya-jun, a new method for studying the unsteady vortex frequency characteristics on rotor blades of turbine engine, *Journal of Experiments in Fluid Mechanics* 20 (2) (2006) 7–11.